

# Implementation of Position Sensorless Control Based on Coordinate Transformation for Brushless DC Motor Drives

Shivanand N Sonnad<sup>1</sup> Manish.G.Rathi<sup>2</sup>

**Abstract**— This paper presents a novel method for sensorless brushless dc (BLDC) motor drives, Based on the characteristics of the back electromotive force (EMF), the rotor position signals would be constructed. It is intended to construct these signals which make the phase difference between constructed signals and back EMF controllable, then rotor position error can be compensated by controlling the phase difference angle in real time. In this paper, the rotor position detection error is analyzed. Experiments are implemented on a 16F877A Microcontroller chip as a control core to demonstrate the feasibility of suggested sensorless control.

**Key words:** Brushlessdc (BLDC) motor, compensate, coordinate transform, sensorless, rotor position-detection error.

## I. INTRODUCTION

In recent years, the permanent magnet (PM) brushless dc motor (BLDC) is receiving much interest in automotive computer, industrial and household products, etc. due to its high efficiency, compact size, lower maintenance and ease of control. The three-phase wye-connected BLDC motors are usually supplied with a six-step  $2\pi/3$  inverter and for assuring the normal system operation, the rotor position signals are necessary. Traditionally, a rotor position sensor such as hall element is used for detecting the rotor position in BLDC motor due to its simplicity and low cost. However, the rotor position sensors show disadvantages from the standpoint of total system cost, size and reliability (2) consequently, for eliminating these sensors from motor, many research workers have attempted to control the speed of BLDC motors without rotor position sensors or speed sensors (3).

In this paper, taking a surface-mounted Permanent Magnet BLDC motor as the research object, of which the air-gap flux has a trapezoidal shape, new sensorless-control method is proposed. It is based on coordinate transformation. In order to compensate the rotor-position detection error and obtain the commutation sequences, two coordinates are defined, which are named as "a" and "b". For compensating the error, the angle  $\beta$ , which is between "b" coordinate and "a" coordinate, respectively is controlled in real time and zero-crossing instants of constructed position signals that are the projections on "b" coordinate from "a" coordinate, are just the phase commutation instants. The proposed method only needs two-phase terminal voltage signals, not to simulate the neutral voltage of the motor, and the detection error could be compensated in real time. Consequently, it is more suitable for the wide speed range.

## II. TRADITIONAL SENSORLESS METHOD

Generally, there are three parts for sensorless BLDC motor drives, which are the inverter, the back EMF detection circuit, and the control unit, respectively, as shown in Fig

2.1. In this section, the error compensation methods are reviewed, and the rotor-position-detection error is analyzed.

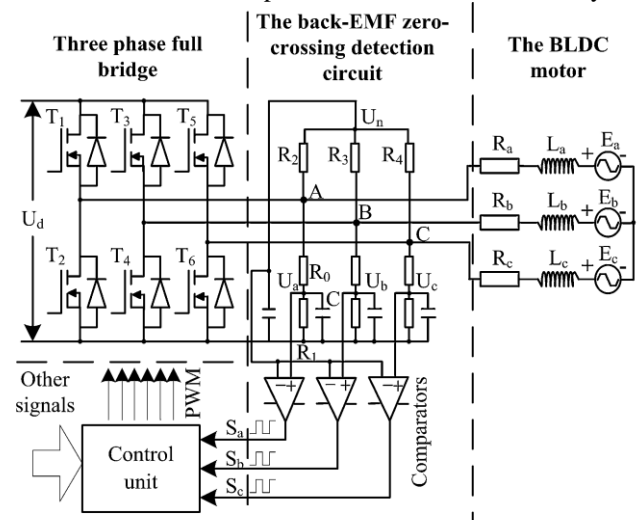


Fig.1: Phase-voltage method (PVM) drive system.

As shown in Fig.2.1, the back EMF zero-crossing detection circuit is composed of four parts, including the resistance network, dividing voltage circuit, first-order low pass filter and comparators in the PVM.  $R_2, R_3$  and  $R_4$  constitute the resistance network which is used for simulating the motor neutral point voltage if the neutral wire of the BLDC motor is not available.  $R_0$  and  $R_1$  constitute the dividing voltage circuit, which is used to reduce the terminal voltage so that the signal is sampled between  $+15\text{v}$  and  $-15\text{v}$  if the comparators are supplied by the  $+15\text{v}$  power source. The voltage dividers and the capacitances constitute the low pass filters. The filters have two functions as follows; 1) eliminating the chopped pulses caused by the pulse width modulation (PWM) operation, appearing along with the back EMF, and 2) making the back emf delay by  $\pi/6$  electrical radians at the rated speed, in order to obtain commutation timing. The comparators are used for generating the rotor position pulse signals, by comparing  $U_a, U_b$ , and  $U_c$  to  $U_n$ . If  $U_a$  is greater than  $U_n$ , then the comparator outputs high level, else the comparator outputs low level, which is expressed as  $S_a$  in figure 2.1. At the rising edge of  $S_a$ , the MOSFET T1 is on and MOSFET T5 is off. At the falling edge of  $S_a$ , the MOSFET T2 is on and the MOSFET T6 is off. Similarly, according to the rising and falling edges of  $S_b$  and  $S_c$ , other commutation instants could be obtained.

### A. Analysis Of The Rotor-Position-Detection Error.

In a PM BLDC motor, the transient value of flux linkage in each phase winding is directly related to the rotor position. However, the back EMF is due to the rate of change of flux linkages, which is mainly excited by the PM on the surface of the rotor; hence, the back EMF can be indirectly related to the rotor position, and used for position sensorless control. For implementing the proposed method, the 16F877A Microcontroller chip is used.

**B. Error Caused By The Low-Pass Filters.**

Usually, the terminal or phase voltages are used for sensorless control, as the back EMF is difficult to be detected directly. The terminal voltage is the combination of dc and harmonic components generated by PWM operation. The magnitude of the dc component varies directly with the duty cycle of PWM, and the frequencies of harmonic components are multiples of the carrier frequency. For extracting the back EMF, there may be low-pass filters to eliminate the chopped pulses from the terminal voltages. The parameters of the filters would be usually designed according to the rated rotation speed of the prototype.

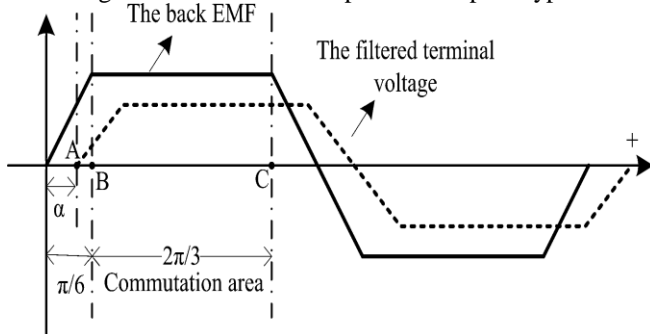


Fig. 2: Commutation instant for the normal rotation  
The phase-response function of the adopted low-pass filter is given

$$\alpha(\omega) = \tan^{-1} \frac{R_0 R_1 C \omega}{R_0 + R_1} \dots (1)$$

where  
R0 = 20 kΩ , R1 = 2 kΩ the divider resistors;  
C = 0.47 μF the filter capacitor;  
ω = 2πf the angular frequency and f is the fundamental frequency.

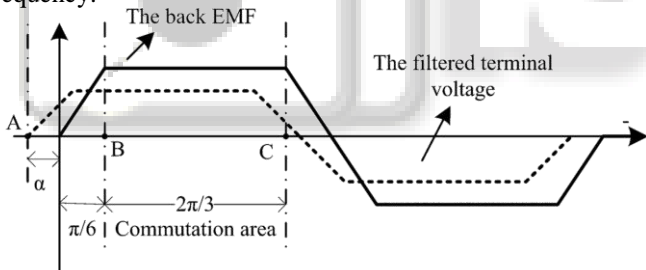


Fig. 3: Commutation instant for the reversing rotation  
The phase shift depends on the speed of the rotor. However, the winding current should be commutated at π/6 (electrical degrees) lagged behind back EMF zero-crossing point hence, the error due to filters under different speeds should be taken into account. Fig. 2.2 shows the back EMF, the filtered terminal voltage, and the commutation instant. The commutation instant should be the time that lags behind the zero-crossing point of the back EMF by π/6, e.g., the B point as shown in Fig. 2.3 The filtered terminal voltage lags behind the back EMF by the angle α, which could be calculated by equation(1), assuming that the position detection errors, due to the armature reaction, sampling, and the uncertainty of the devices, are negligible. For the normal rotation, the filter is usually designed to make the filtered terminal voltage lag behind the back EMF by π/6 at the rated speed, and the commutation instant is just the zero-crossing point of the filtered terminal voltage, but at the other speed, α is not π/6. If n (the rotation speed) is lower than nN (the rated speed), then α is smaller than π/6, else if n

is higher than nN , then α is larger than π/6. As shown in Fig. 2.2 from 0 to nN , A point approaches to B point, whereas it is further away from B point under reversion rotation as shown in Fig.2.3. Consequently, the commutation instant should lag behind the zero-crossing point of the filtered terminal voltage by the angle β as expressed in equation (2).

$$\beta = \begin{cases} \frac{\pi}{6} - \alpha(\omega), & \text{(for natural operation)} \\ \frac{\pi}{6} + \alpha(\omega), & \text{(for reverse operation)} \end{cases} \dots (2)$$

**III. PROPOSED ARITHMETIC FOR SENSORLESS BLDC DRIVES**

**A. Constructed Position Signals Based On Coordinate Transformation**

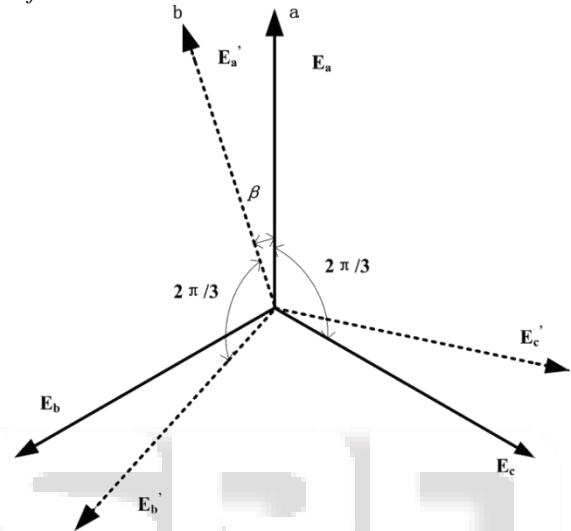


Fig. 4: Coordinate transformation.

In this section, two coordinates are defined, which are named as “a” and “b,” as shown in Fig. 3. The angle β is between “b” coordinate and “a” coordinate, respectively. E<sub>a</sub>, E<sub>b</sub>, and E<sub>c</sub> are the three-phase filtered-terminal voltages, which are defined in “a” coordinate. The projections on “b” coordinate from “a” coordinate are defined E<sup>1</sup><sub>a</sub>, E<sup>1</sup><sub>b</sub>, E<sup>1</sup><sub>c</sub>. To begin with, the phase relationship between E<sup>1</sup><sub>a</sub> and E<sub>a</sub> characteristics of E<sup>1</sup><sub>a</sub> will be analyzed. Then, Fourier expansions for E<sub>a</sub>, E<sub>b</sub>, and E<sub>c</sub> are given as in equation (3) .

$$\begin{aligned} E_a &= \frac{U_d}{2} + \sum_{n=1}^{\infty} (a_n \cos[n\omega t] + b_n \sin[n\omega t]) \\ E_b &= \frac{U_d}{2} + \sum_{n=1}^{\infty} \left( a_n \cos n[\omega t + \frac{2\pi}{3}] + b_n \sin n[\omega t + \frac{2\pi}{3}] \right) \\ E_c &= \frac{U_d}{2} + \sum_{n=1}^{\infty} \left( a_n \cos n[\omega t - \frac{2\pi}{3}] + b_n \sin n[\omega t - \frac{2\pi}{3}] \right) \end{aligned} \dots (3)$$

where U<sub>d</sub> is the dc bus voltage The projections on “b” coordinate from “a” coordinate are given in (4). The mathematical expression of E<sup>1</sup><sub>a</sub> as given in (5) is obtained by substituting (3) into (4). From (5), the characteristics of E<sup>1</sup><sub>a</sub> can be seen as expressed in (6). From (6), the characteristics of E<sup>1</sup><sub>a</sub> can be summarized as follows: 1) the dc component is eliminated; 2) the 3nth harmonic is eliminated and 3) E<sup>1</sup><sub>a</sub> is just the fundamental wave if the fifth harmonic component and other higher harmonic components can be neglected, and the phase difference between E<sup>1</sup><sub>a</sub> and the fundamental component of e<sub>a</sub> is just the

angle  $\beta$ , which can be controlled in real time. According to the three phase symmetric relationship,  $E_b^1$ ,  $E_c^1$  also have these characteristics.

$$E_a^1 = E_a \cos \beta + E_b \cos\left[\frac{2\pi}{3} - \beta\right] + E_c \cos\left[\frac{2\pi}{3} + \beta\right]$$

$$E_b^1 = E_b \cos \beta + E_c \cos\left[\frac{2\pi}{3} - \beta\right] + E_a \cos\left[\frac{2\pi}{3} + \beta\right]$$

$$E_c^1 = E_c \cos \beta + E_a \cos\left[\frac{2\pi}{3} - \beta\right] + E_b \cos\left[\frac{2\pi}{3} + \beta\right]$$

..... (4)

$$E_a^1 = \sum_{n=1}^{\infty} a_n \left( 2 \cos \beta \cos[n\omega t] \sin\left[\frac{n\pi}{3}\right]^2 - \sqrt{3} \sin \beta \sin\left[\frac{2n\pi}{3}\right] \sin[n\omega t] \right) + b_n \left( \sqrt{3} \sin \beta \sin\left[\frac{2n\pi}{3}\right] \cos[n\omega t] + 2 \cos \beta \sin[n\omega t] \sin\left[\frac{n\pi}{3}\right]^2 \right)$$

$$\begin{cases} E_a^1(0) = 0 \\ E_a^1(1) = \frac{3}{2} (a_1 \cos[\beta + \omega t] + b_1 \sin[\beta + \omega t]) \dots\dots(6) \\ E_a^1(3n) = 0 \end{cases}$$

Where

$E_a^1(0)$  is the dc component of  $E_a^1$ ,  $E_a^1(1)$  is the fundamental component of  $E_a^1$  and  $E_a^1(3n)$  is the  $3n^{\text{th}}$  ( $n = 1, 2, 3, \dots$ ) harmonic components.

The back EMF, which is trapezoidal, contains only odd harmonics. Therefore, the phase of  $E_a^1$  is the same as the fundamental phase of  $E_a$ . The advantages of the proposed arithmetic can be summarized as follows: 1) using the angle  $\beta$ , the rotor position-detection error could be compensated; 2) the neutral point voltage in PVM Because the dc component is eliminated by the coordinate transform, the zero-crossing points of  $E_a^1$  can be used for commutation; and 3) it can be seen that the amplitude of  $E_a^1$  is 1.5 times the amplitude of the fundamental of  $E_a$ , which enables better estimation of the zero-crossing points than conventional methods  $E_a^1$ , could be regarded as fundamental wave if the higher harmonics are neglected.

**B. Hardware Implementation**

The proposed sensorless BLDC motor drive system could be designed as shown in Fig. 3.2. In comparison with Fig 2.1, the back EMF zero-crossing detection circuit is substituted by the back EMF sampling circuit, which includes the low-pass filters, the sampling circuit, and the regulation circuit. The filters are used for eliminating the chopped pulse caused by the PWM operation. The sampling circuit, which is galvanically isolated from the Microcontroller would sample the filtered terminal voltage to the regulation circuit, and the regulation circuit would scale down the filtered terminal voltage between 0 and +3 V, which could be read by the Microcontroller. For simplifying the hardware circuit, the phase C terminal voltage is not sampled, which could be reconstructed by  $E_a$  and  $E_b$  according to the three-phase symmetry property. It could be easily implemented by programming.

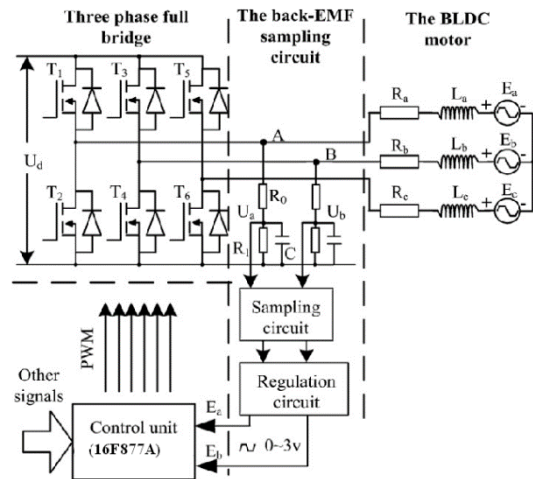


Fig. 5: Proposed Sensorless BLDC Motor-Drive System

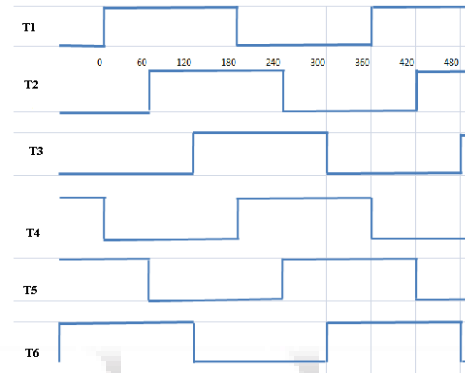


Fig. 6: Switching Sequences Of 6 Mosfet's(180° Conduction Mode and these pulses are fed to bldc motor)

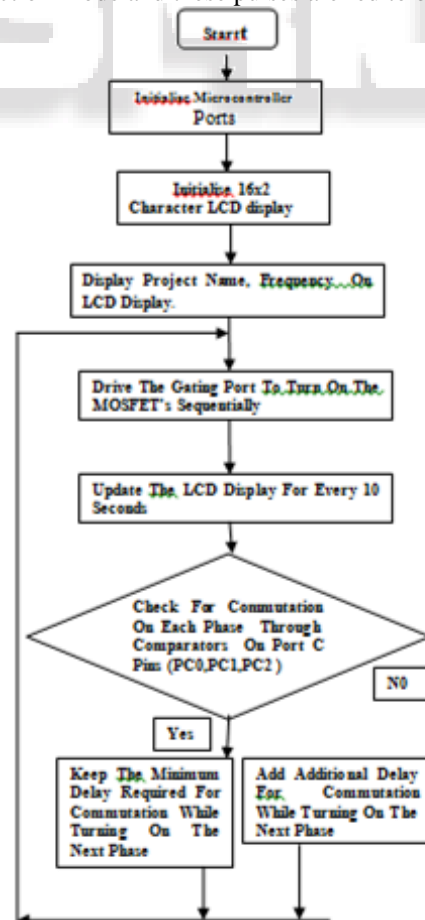


Fig. 7: Software flowchart

#### IV. EXPERIMENTAL RESULTS

The proposed arithmetic for sensorless BLDC motor drive has been successfully implemented on the experimental BLDC motor, and its specification is shown in table 1.

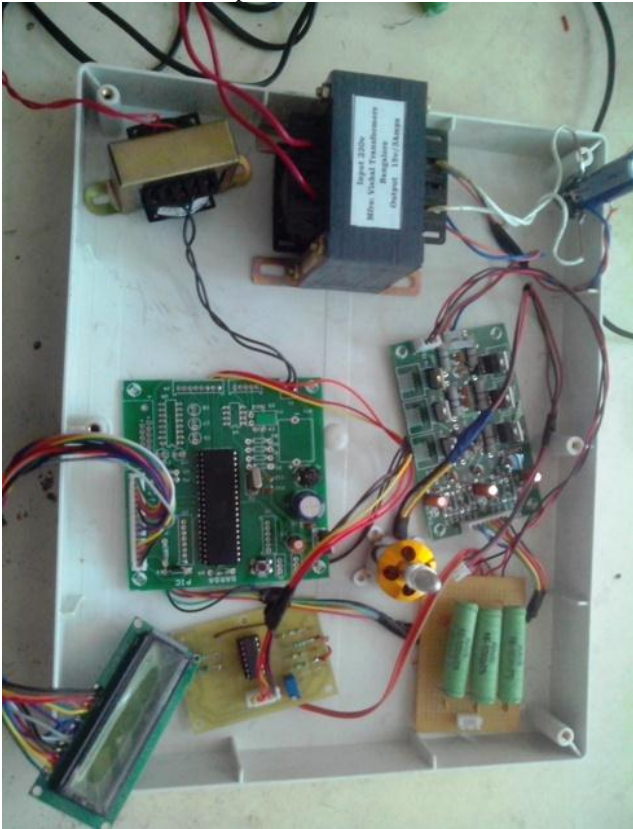


Fig. 8: photograph of complete hardware set up.

**Table - 1**  
**Motor Parameters**  
**3 phase BLDC motor**

Rated DC voltage(v)	- 25
Rated speed(rpm)	- 750
Number of phases	-3
Number of poles	-4
Output power(w)	- 60

#### V. CONCLUSION

A novel arithmetic for sensorless BLDC motor drives has been presented in this paper. The rotor-position signals, e.g.,  $E_a^1$ ,  $E_b^1$ , and  $E_c^1$  are constructed by the two-phase terminal voltages, which can be used for commutation. The proposed sensorless-control method has the following advantages: 1) it only needs two-phase terminal voltage signals, without using the neutral voltage signal of the motor and 2) in order to obtain the commutation instants, the rotor-position-detection error could be calculated in real time, and compensated by computing the angle  $\beta$ , over the speed range. Experimental results are verified by the hardware.

#### REFERENCES

[1] T.H.Kim.H.W.Lee, and M.Ehsani,"State of the art and future trends in position sensorless brushless DC motor drives." In Proc.31<sup>st</sup> Annu.Conf and Ind.Electron.Soc.,2005.p.8

- [2] K.Y.Chen and Y.Y.Tzou,"Design of a sensorless commutation IC for BLDC motors,"IEEE Trans.Power Electron.,vol 18,no.6.pp.1365-1375,Nov.2003
- [3] S. Ogasawara and H. Akagi,"An approach to position sensorless drive for brushless DC motors."IEEE Trans ,Ind.Appl.,vol.27.no.5.pp.928-933.Sep.1991
- [4] Modern Power Electronics and Ac drives By Bimal K.Bose.
- [5] Abolfazl Halvaei Niasar, Abolfazl Vahedi, And Hassan Moghbelli, "A Novel Position Sensorless Control Of A Four-Switch, Brushless DC Motordrive Without Phase Shifter " IEEE Transactions On Power Electronics, Vol. 23, No. 6, November 2008.
- [6] Aakanksha Girokar , G. Bhuvaneshwari , "Control of PMBLDC Motor Using Back EMF Sensing with Adaptive Filtering" International Conference on Computer Communication and Informatics (ICCCI -2013), Jan. 09 – 11, 2013, Coimbatore, INDIA
- [7] Tae-Won Chun , Quang-Vinh Tran, Hong-Hee Lee and Heung-Geun Kim, "Sensorless Control of BLDC Motor Drive for an Automotive Fuel Pump Using a Hysteresis Comparator" 2013 IEEE.
- [8] Yoko Amano ,Toshio Tsuji, Atsushi Takahashi, Shigeo Ouchi,Kyoji Hamatsu,And Masahiko Iijima- "A Sensorless Drive System for Brushless DC Motors Using a Digital Phase-Locked Loop" Translated from Denki Gakkai Ronbunshi, Vol. 121-D, No. 11, November 2001, pp. 1155–1162.
- [9] P. Devendra1, Madhavi TVVS, K Alice Mary and Ch. Saibabu "Microcontroller based control of three phase bldc motor"- Journal of Engineering Research and Studies Vol. II/ Issue IV/October-December, 2011.
- [10] Cheng-Tsung Lin, Chung-Wen Hung, and Chih-Wen Liu, "Position Sensorless Control for Four-Switch Three-Phase Brushless DC Motor Drives-IEEE Transactions On Power Electronics, Vol. 23, No. 1, January 2008